

Scalar and Vector Leptoquark Pair Production at Hadron Colliders: Signal and Backgrounds

B. Dion, L. Marleau and G. Simon
Département de Physique, Université Laval
Québec QC Canada, G1K 7P4
(1998)

Abstract

We perform a systematic analysis of scalar and vector leptoquark pair production at the Fermilab Tevatron and at the CERN LHC. We evaluate signal expectations and background levels for the processes $pp(p\bar{p}) \rightarrow 2 \text{ jets} + e^+e^-$ and $2 \text{ jets} + e + \cancel{p}_T$. The Monte Carlo event generator ISAJET is used to simulate the experimental conditions at the current ($\sqrt{s} = 1.8 \text{ TeV}$, $\mathcal{L} = 100 \text{ pb}^{-1}$) and upgraded ($\mathcal{L} = 2 \text{ fb}^{-1}$) Tevatron as well as the LHC ($\sqrt{s} = 14 \text{ TeV}$, $\mathcal{L} = 10 \text{ fb}^{-1}$). Depending on the luminosity, and assuming a branching ratio $B(LQ \rightarrow eq) = 0.5$, we find a discovery reach up to 170 (255) GeV for scalar leptoquarks at the current (upgraded) Tevatron. Similarly, we find vector leptoquarks to be detectable at masses below 300 (400) GeV depending on the coupling. At the LHC, the discovery reach is enhanced to 1 TeV for scalar leptoquarks and to 1.5 TeV for vectors.

PACS numbers: 11.25.Mj, 13.85.Qk, 14.80.-j.

I. INTRODUCTION

Leptoquarks are color-triplet particles carrying both baryon and lepton quantum numbers which mediate transitions between the quark and lepton sectors. They appear in many extensions of the Standard Model (SM) such as composite models [1] which postulate a common preonic substructure to quarks and leptons, Grand Unified Theories [2,3] which treat quarks and leptons on the same basis, superstring-inspired E_6 models [4,5] and strongly-coupled Abbott-Fahri models [6]. They arise as scalar ($S = 0$) as well as vector ($S = 1$) or even fermionic ($S = 1/2$) particles depending on the model considered. Leptoquarks could be produced in e^+e^- [7,8,9,10], $e\gamma$ [11], ep [12,13,14] and hadron colliders [15,16,17,18,19,20].

Recently, the H1 [13] and ZEUS [14] experiments at HERA have reported an excess of large Q^2 deep inelastic scattering events compared to QCD expectations. One possible explanation which has been put forward to account for these events is that they arise from the single production of a ~ 200 GeV leptoquark. The statistics for these high- Q^2 events remain quite low for now (H1 finds 8 events leading to a leptoquark mass $M \sim 200$ GeV while ZEUS finds 4 events with $M \sim 220$ GeV) and the latest results from both collaborations [21] seem to indicate no significant deviations from Standard Model expectations in the 1997-1998 run. It nonetheless seems worthwhile to investigate the discovery potential of both scalar and vector leptoquarks of such mass at the Tevatron and at the CERN LHC especially since their production in pairs at hadron colliders is almost insensitive to an unknown Yukawa coupling.

In addition, leptoquark searches are also going on at the Fermilab Tevatron and at LEP. For instance, the OPAL collaboration [8] at LEP recently fixed a limit of $M_{LQ} \geq 131$ GeV for scalar leptoquarks of the first generation. Similarly, the OPAL [9] and L3 [10] collaborations have investigated the indirect production of scalar and vector leptoquark in the t -channel and as contact interactions in the $e^+e^- \rightarrow q\bar{q}$ channel. Their results are expressed in terms of the ratio M_{LQ}/λ where λ is the Yukawa coupling of the leptoquark to the quark-lepton pair. They find a limit $\lambda/e \leq 0.2 - 0.7$ for leptoquarks of mass ~ 200 GeV. On the other hand, the latest results from the CDF [15] and D0 [16] collaborations at the Tevatron exclude scalar leptoquarks with masses below 225 GeV and 204 GeV for branching ratios of the leptoquarks to the electron equal to 1 and 0.5 respectively. Making use of their published search for the superpartner of the top quark, the D0 collaboration has also looked for leptoquarks which decay exclusively into neutrinos. Their analysis yields a limit of 79 GeV in this case.

Previous studies have suggested that present Tevatron data [16] most likely excludes vector leptoquarks with masses below 250 GeV. However, a comprehensive study of the various Standard Model backgrounds and the extent to which the signal of a 200-250 GeV leptoquark will be reduced by the kinematic cuts imposed on these backgrounds was still lacking up to now. This motivated an important part of the work presented in this paper, i.e. to present such an analysis and evaluate the vector leptoquark discovery reach at the Tevatron and the LHC. For that purpose, we implement vector leptoquark data and related cross sections in the ISAJET [22] event generator and evaluate the importance of the LQ signal and the SM backgrounds. The ISZRUN package contained in the ZEBRA version of ISAJET is used to perform the selection cuts.

Earlier analyses on pair production of leptoquarks at hadron are available. Only some aspect or conditions have been examined. For example, the authors have analyzed the

pair production of scalar leptoquarks at hadron colliders [23,24] focussing on the cleanest of the possible signatures, i.e. 2 jets $+e^+e^-$. Similarly, other contributions examined pair and single production of scalar leptoquarks at the LHC [25] and single production of scalar and vector leptoquarks through effective photon approximations at the LHC [26]. In this paper, we investigate the ability of the Fermilab Tevatron and at the CERN LHC to observe the pair production of both scalar and vector leptoquarks. We perform a comprehensive analysis which includes the evaluation of the cross section as well as the optimization of the signal-to background ratio through the use of selection and kinematic cuts. We assume a branching ratio $B(LQ \rightarrow eq) = 0.5$ and consider the following two signatures for leptoquark pair production: 2 jets $+e^+e^-$ or 2 jets $+e + \cancel{p}_T$. Finally, we estimate the discovery reach of scalar and vector leptoquarks at the Tevatron and at the LHC.

II. EVENT SIMULATION

The Monte-Carlo event generator ISAJET is used to model the experimental conditions at the Tevatron and at the LHC. The toy detector used for the Tevatron is loosely based on the D0 and CDF detectors at Fermilab. The calorimeter is segmented in cells of size $\Delta\eta \times \Delta\phi = 0.1 \times 0.0875$ with η coverage $-4 < \eta < 4$, where η is the rapidity and ϕ is the azimuthal angle. The hadronic energy resolution is defined such as the jet resolution is $70\%/\sqrt{E}$ while the electromagnetic energy resolution is $15\%/\sqrt{E}$.

The experimental conditions at the LHC are also simulated, with the ATLAS [27] and CMS [28] detectors in mind. The calorimeter is divided in cells of dimension $\Delta\eta \times \Delta\phi = 0.05 \times 0.05$, with a rapidity range of $-5 < \eta < 5$. The hadronic energy resolution is given by

- $50\%/\sqrt{E} \oplus 0.03$ for $-3 < \eta < 3$,
- $100\%/\sqrt{E} \oplus 0.07$ for $3 < |\eta| < 5$.

The electromagnetic energy resolution is given by $10\%/\sqrt{E} \oplus 0.01$ independently of the rapidity.

Jets are found using a fixed cone algorithm with radius $R = \sqrt{(\Delta\eta)^2 + (\Delta\phi)^2} = 0.7$. The jet energy scale is set by requiring

- a transverse energy $E_T > 15$ (50) GeV at the Tevatron (LHC)
- a pseudorapidity $|\eta_j| \leq 1.5$.

On the other hand, electrons are required to

- be separated from any jet by $\Delta R \geq 0.3$
- have a transverse momentum $p_T > 20$ (100) GeV at the Tevatron (LHC)
- have a pseudorapidity $|\eta_e| \leq 1.5$.

The calculations are performed using the CTEQ3M parton parametrization [29]. Higher-order corrections to the cross section are available for pair of scalar leptoquarks [30]. The calculations presented here always assume the lowest-order cross sections. Higher-order corrections could be applied in the form of a K -factor whenever available.

III. SIGNAL AND BACKGROUNDS

A. Leptoquark signal

For the purposes of this work, we do not focus on any specific model and consider the production of generic first-generation leptoquarks which can be of type (eu) (with electric charge $Q = \pm\frac{1}{3}, \pm\frac{5}{3}$) or (ed) (with $Q = \pm\frac{2}{3}, \pm\frac{4}{3}$) which decay into an electron and a quark or into a neutrino and a quark with equal branching ratios $B(LQ \rightarrow eq) = B(LQ \rightarrow \nu q) = 0.5$ or in an electron and a quark with $B(LQ \rightarrow eq) = 1$. After hadronization and fragmentation, the expected signatures for leptoquark pair production consist of two (or more) jets along with two electrons, one electron and a missing transverse momentum or simply a missing transverse momentum.

Leptoquark pair production occurs via two dominant subprocesses, $q\bar{q}$ annihilation or gluon fusion (see Fig.1 for the Feynman diagrams). The only model-dependent parameter is the Yukawa coupling which appears in the t -channel diagram in $q\bar{q}$ annihilation. Low-energy data as well as collider experiments constrain this coupling to be of the order of electric strength or lower. In this case, the contribution coming from this diagram becomes negligible with respect to the others. Consequently, the corresponding contribution is not included in the cross section. This absence of sensitivity to the magnitude of the Yukawa coupling, along with the large center-of-mass energy, is one of the main reasons why it is worthwhile to investigate pair production of leptoquarks in hadron colliders.

The cross sections for both scalar and vector leptoquark pair production in hadron colliders have been extensively reviewed [18,19,20]. In the scalar case, the leptoquark coupling to the gluon is simply given by the strong coupling. There is however an ambiguity in the vector case. In order to evaluate the $q\bar{q}, gg \rightarrow VV$ cross sections both the trilinear gVV and the quartic $ggVV$ couplings need to be evaluated. In any model in which vector leptoquarks appear as fundamental objects, they correspond to the gauge bosons of an extended gauge group. In this case both couplings are fixed by gauge invariance. However, there is a possibility that vector leptoquarks arise as a low-energy manifestation of a more fundamental theory at larger scale, in which case some anomalous couplings may appear. One such coupling comes from the ‘‘anomalous magnetic moment’’, usually described by the parameter κ and which takes unit value in the gauge theory case. The Lagrangian takes the form:

$$\mathcal{L}_V = -\frac{1}{2}F_{\mu\nu}^\dagger F^{\mu\nu} + M_V^2 V_\mu^\dagger V^\mu - ig_s \kappa V_\mu^\dagger G^{\mu\nu} V_\nu \quad (1)$$

where $G_{\mu\nu}$ is the usual gluon field strength tensor, V_μ is the leptoquark field and $F_{\mu\nu}^\dagger = D_\mu V_\nu - D_\nu V_\mu$. One might also include an anomalous electric quadrupole moment [20] usually described by the variable λ and which takes the value $\lambda = 0$ in the gauge case. Here, for the sake of clarity, we present our analysis for only two specific cases: $\kappa = \lambda = 0$ (minimal coupling) and $\kappa = 1, \lambda = 0$ (gauge coupling). The cross section for vector leptoquark pair production at hadron colliders has previously been calculated for various sets of parameters κ and λ [20]. For $\lambda = 0$, the results show that the cross section is largest in the gauge case ($\kappa = 1$) and reaches a minimum for values of $\kappa \sim 0$. Both differ by a factor somewhat less than an order of magnitude. By comparison, the cross section for pair production of scalar

leptoquark turns out to be smaller by a factor of $\sim 2 - 3$ compared with vector leptoquarks with minimal coupling.

B. SM Backgrounds

The main sources of background to leptoquark pair production as identified by [18,19] are (1) gauge boson production involving the production of two jets, (2) QCD processes involving the production of heavy flavors (b , c) and (3) $t\bar{t}$ production.

1. Gauge boson production

The main background to leptoquark pair production at the Tevatron comes from $Z^* + 2$ jets (Fig.2(a)) in the dielectron channel and from $W^* + 2$ jets (Fig.2(b)) in the electron plus missing transverse energy channel [15,16,23,24,25]. In the latter case, the source of hard electrons comes from the leptonic decay of the gauge bosons while the jets typically arise from gluon radiation from incoming partons. Although potentially large, this background can be reduced by an invariant mass cut on the lepton pair (dielectron case) or a transverse mass cut on the lepton and missing p_T (single electron case). The present analysis will show that this background can also be reduced by kinematic cuts on the transverse energy of the jets and leptons.

2. QCD processes

Background from QCD processes (Fig.2(c)) arise from the hadroproduction of heavy quarks c and b . Note that the top quark is not included in this list. The wide difference in mass results in a completely distinct signature and topology and the top quark will be dealt with separately. Relevant QCD processes include pair production ($c\bar{c}$, $b\bar{b}$), single production (cq , cg , bq , bg) and gluon pair production with one of the gluons leading to $c\bar{c}$ or $b\bar{b}$. This background can in principle be important as the relative cross sections are very large. However, a great majority of QCD events can be eliminated by adequate cuts. In particular, QCD events typically have much lower transverse momentum distributions than $t\bar{t}$ and leptoquark production events. This is particularly true in the case of the leptons which in this case arise from the semileptonic decay of the c and b hadrons.

3. $t\bar{t}$ background

Pair production of top quarks (Fig.2(d)) will certainly be a dominant source of background at the LHC. This background implies the semileptonic decay of one of the quarks into a b quark, an electron and a neutrino, ν_e . This process is characterized by a missing transverse momentum, which implies that the electron energy is lower than that of the corresponding jet. Another potential background comes from the single production of a top quark accompanied by a quark or a gluon ($tq(g) \rightarrow tq(g)$). However, previous results have shown [25] this background to be negligible with respect to the pair production channel. The value $M_t = 175$ GeV is assumed for the top mass.

IV. SELECTION CUTS

Leptoquark pair production events are generated assuming a branching ratio $B(LQ \rightarrow eq) = 0.5$ unless stated otherwise and classified according to the number of jets and of isolated leptons present in each event. As discussed above, the signature to leptoquark pair production can consist of

- (a) 2 jets + e^+e^- (dielectron channel),
- (b) 2 jets + $e + \cancel{p}_T$ (single electron channel),
- (c) 2 jets + \cancel{p}_T (missing p_T channel).

Typically, channels (a) and (c) occur 25% of the time while channel (b) occurs with a 50% probability. The jets and leptons are expected to be emitted in the central rapidity region with high transverse energy. Leptoquark events originating from signal (c) tend to be overwhelmed by the QCD background coming from $q\bar{q}$ and gluon pair production and do not allow for a clean identification as the lepton-quark invariant mass cannot be reliably calculated in this case. Consequently we restrict ourselves to signals (a) and (b). This means that $\sim 75\%$ of all the leptoquark pair production events can contribute to the final results while the other 25% are lost.

The selection cut on the events corresponding to channel (a) is made by requiring

1. two isolated electrons with a transverse energy $E_T > 20$ (100) GeV and a pseudorapidity $|\eta_e| \leq 1.5$ at the Tevatron (LHC),
2. at least two jets with a transverse energy $E_T > 15$ (50) GeV and a pseudorapidity $|\eta_j| \leq 1.5$ at the Tevatron (LHC).

Events corresponding to channel (b) are required to contain

1. one isolated electron with a transverse energy $E_T > 25$ (100) GeV and a pseudorapidity $|\eta_e| \leq 1.5$ at the Tevatron (LHC),
2. at least two jets with a transverse energy $E_T > 25$ (50) GeV and a pseudorapidity $|\eta_j| \leq 1.5$ at the Tevatron (LHC).

An optimization is carried out by varying kinematic cuts until they maximize the signal-to-background ratio. The nature and values of those cuts are based on earlier calculations [15,16,17,23,24]. For instance, in order to reduce the background coming from Drell-Yan processes we impose a cut on the invariant mass of the lepton pair. We thus eliminate all events near the Z peak: $82 \text{ GeV} \leq M_{e^+e^-} \leq 100 \text{ GeV}$. We do not apply a transverse mass cut on the lepton and missing p_T to reduce the background from W events in the (b) channel but choose instead to require a missing transverse energy $\cancel{p}_T \geq 40$ (200) GeV at the Tevatron (LHC).

Finally, we impose a cut on the total transverse energy of the jets and leptons as defined by

$$S_T = \sum_j E_T^j + \sum_e E_T^e. \quad (2)$$

Note that the former expression is based on the convention used in [17] and should not be confused with the S_T variable used in other D0 publications which includes the missing transverse momentum. We find the optimal cuts at the Tevatron to be $S_T \geq 200$ and 190 GeV for events corresponding to channel (a) and (b) respectively. Similarly we find $S_T \geq 1.5$ and 1.0 TeV to be optimal at the LHC.

V. LEPTOQUARK PRODUCTION AT THE TEVATRON

The results for the Tevatron are shown in Figs 3-6. Figure 3 displays the missing p_T distributions in the single electron channel for the various backgrounds as well as for vector leptoquarks in the gauge case ($\kappa = 1$). The selection cuts described in Section IV have been applied and the value $B(LQ \rightarrow eq) = 0.5$ has been chosen for the leptoquark branching ratio into an electron and a quark. The corresponding figures for the minimal coupling and scalar cases are not displayed as they are very similar, differing roughly by a constant factor. One sees from Fig. 3 that the background for QCD processes is dominant at small values of \cancel{p}_T , as could be presumed from the large cross section as well as the typically low transverse momentum available for the neutrino in this case. On the other hand, the background from W + jets and Z + jets becomes important at slightly higher values of \cancel{p}_T , around 50 -100 GeV. The background from $t\bar{t}$ is comparatively negligible and is practically invisible in Fig.3. The \cancel{p}_T distribution of the leptoquark signal shows an approximately constant behavior for values of $\cancel{p}_T \leq 150$ GeV and gradually decreases for higher values. In order to reduce the QCD background sufficiently without significantly reducing the signal, we impose a cut of 40 GeV on \cancel{p}_T .

Figure 4 shows the S_T distribution for the signal as well as the various backgrounds once the \cancel{p}_T cut has been applied. Both single electron and dielectron channels have been included in this graph. Once again, only the results for the gauge case are displayed. Clearly, the W + jets, Z + jets and QCD backgrounds, though very important, are peaked at small values of S_T (~ 100 GeV for W, Z + jets and ~ 150 GeV for QCD) while the leptoquark peak is wider and concentrated at higher values of S_T . Roughly, one can see that the peak corresponds typically to twice the leptoquark mass, especially for leptoquark masses approaching the kinematic limit of the collider. This is to be expected as the lepton-quark transverse energy then corresponds approximately to the leptoquark mass. An interesting feature is that the peak widens as the leptoquark mass increases. This feature is largely due to the increasing jet multiplicity at higher values of the leptoquark mass. For instance, about 40% of the events corresponding to $M_{LQ} \geq 250$ GeV contain 3 or 4 jets while this proportion is about 25% for masses below 200 GeV. These excess jets, which are emitted in the fragmentation/hadronization phase of the event, escape with a fraction of the available transverse energy and cause the observed smearing. We find the overall optimal cut to be of 190 GeV for the single electron channel and 200 GeV for the dielectron channel.

Figure 5 (a-c) displays the invariant mass distribution of both signal and background for $\cancel{p}_T > 200$ GeV and $S_T > 190$ (200) GeV for the single electron (dielectron) channel. The lepton-jet pairing algorithm is based on the transverse energy of the quarks and leptons.

Specifically, the largest- p_T electron is paired with the lowest- E_T jet and vice-versa. For single-electron events, the same approach is applied with the \cancel{p}_T used as corresponding to the neutrino transverse energy. This figure shows the strong quark-lepton correlation in the leptoquark signal. The mass peak is quite narrow and allows for a straightforward identification of the leptoquark mass.

One can see from Fig. 5 that the background is dominated by $W, Z + \text{jets}$ processes which come mostly from the production of a W^\pm in the single-electron channel and from Z^0 in the dielectron channel. Note that transverse mass cuts can also be applied to reduce the background from $W + \text{jets}$ [16]. However, the application of this cut seems unnecessary here as the background is most important only at small values of the quark-lepton invariant mass ($\sim 75 - 150$ GeV). On the other hand, backgrounds from QCD and $t\bar{t}$ production are relatively small and are also concentrated at small values of the invariant mass. Leptoquarks of masses 200-250 GeV and higher are thus virtually background-free.

The leptoquark discovery reach at the Tevatron in the scalar as well as in the vector cases can be read directly from Fig. 6. In this figure, the partial cross section for leptoquark pair production is displayed. This graph is obtained by integrating over the lepton-jet invariant mass peak for the whole range of leptoquark masses. For leptoquarks of mass lower than 200 GeV, we integrate over a bin of width $\Delta M_{ej} = 40$ GeV around the peak while we take $\Delta M_{ej} = 50$ GeV for $M_{LQ} \geq 200$ GeV.

In this figure, both the $B = 0.5$ (Fig. 6 (a)) and $B = 1$ (Fig. 6 (b)) cases are included for the leptoquark branching ratio. A closer look at these graphs reveals that the partial cross section is larger when the branching ratio is equal to unity. This is partly due to the fact that all the leptoquark events observed in this case correspond to the dielectron channel and can thus be included in the final results, in contrast with the $B = 0.5$ case where 25% of the events correspond to the \cancel{p}_T channel (channel (c) of Section IV) and are excluded from the analysis. A second explanation comes from the relative efficiency of the selection cuts to single out events in both channels. Indeed, a thorough analysis of our results indicates that the ratio of events that are selected from the sample tends to be larger in the dielectron channel than in the single electron channel.

The backgrounds are also illustrated in Fig. 6. While the dominant background comes from $W, Z + \text{jets}$ production and QCD processes in the $B = 0.5$ case, the only remaining background when $B = 1$ arises from Drell-Yan production of a $Z + \text{jets}$. In both cases, this background is small in comparison with the signal and is concentrated at small values of the electron-jet invariant mass. We impose a 5σ statistical significance as well as a minimum of 5 events for leptoquark discovery. The integrated luminosity for the Tevatron current run is 100 pb^{-1} and the corresponding limit on the cross section is illustrated by the dashed line of Fig. 6. We find a discovery reach of 170 (175) GeV for scalar leptoquarks with a branching ratio of $B = 0.5$ (1). Comparison with present Tevatron data can be achieved by relaxing the requirements to a 5σ statistical significance relative to the background. Considering the current accumulated luminosities of 123 and 115 pb^{-1} in the dielectron and single electron channels at D0, we find a reach of 205 (215) GeV for $B = 0.5$ (1) in agreement with the results of D0. In the case of vector leptoquarks, the discovery reach for 5 events is enhanced to 225 (235) GeV with the minimal coupling $\kappa = 0$ and 280 (290) GeV with the Yang-Mills coupling $\kappa = 1$ for $B = 0.5$ (1).

It is also interesting to reestimate these bounds in view of the luminosity upgrade which

is supposed to take place when the Main Injector comes into function in 2000-2002. The expected luminosity should reach 2 fb^{-1} [31]. Processes with cross sections above the dotted line of Fig. 6 could then be seen. This allows for a discovery reach of 255 (265) GeV for scalar leptoquarks with a branching ratio of $B = 0.5$ (1). Similarly, we find vector leptoquarks to be detectable up to 315 (325) GeV for a minimal anomalous coupling and 365 (380) GeV for a gauge-like coupling.

VI. LEPTOQUARK PRODUCTION AT THE LHC

The results of our analysis for the LHC are displayed in Figs 7-12. Let us first examine the \cancel{p}_T distribution for backgrounds and vector leptoquark signal in Fig. 7. As above, $B = 0.5$ is used for the branching ratio of the leptoquark into an electron and a quark and only the single electron channel is included in the graph. The main backgrounds can be seen to arise from QCD processes and $t\bar{t}$ production. Backgrounds from W and Z production are eliminated by the selection cuts of Sect. IV. Typically, the electrons emitted in these processes have rather low transverse momentum as can be expected from the fact that the W and Z bosons are generally collinear with the beam. Clearly, this distribution shows that the neutrino emitted in semileptonic decay of c and b hadrons does have a small transverse energy. This background can thus be significantly reduced by applying a \cancel{p}_T cut. The $t\bar{t}$ distribution displayed in the same figure is peaked at higher values and becomes dominant over the QCD background at large \cancel{p}_T . In contrast, the neutrinos which originate from leptoquark decay typically possess a much larger transverse energy independently of the leptoquark mass. This is explained by the fact that the neutrino radiated by the W boson in the decay of the top quark shares the available transverse energy with an electron while the whole transverse energy is transmitted to the neutrino in leptoquark decay. On the other hand, the \cancel{p}_T distribution of the leptoquark signal is approximately constant up to ~ 1 TeV for $M_{LQ} = 750$ GeV and higher for $M_{LQ} \geq 1$ TeV. A \cancel{p}_T cut of 200 GeV is adequate to optimize the signal-to-background ratio.

Figure 8 shows the S_T distribution for QCD and $t\bar{t}$ background as well as for gauge-like vector leptoquarks of masses 750, 1000 and 1250 GeV. One sees from this figure that the main backgrounds originate from QCD events and from $t\bar{t}$ production. The leptoquark signal is clearly dominant independently of the S_T cut. This is in contrast to the Tevatron case where this cut was essential to discriminate the signal from the (mostly electroweak) background. This domination of the leptoquark signal is caused by the \cancel{p}_T cut of 200 GeV we have applied beforehand. Finally, one sees once again that the S_T distribution for the background is peaked at significantly smaller values than the signal. The peak is located in both background cases at values around 1 TeV while the signal is characterized by a wider distribution peaked at values over 2 TeV. Clearly, a S_T cut of ~ 2 TeV would be sufficient to eliminate the background completely. However, such a cut would also reduce the signal-to-background ratio as the leptoquark signal takes relatively large values in part of this range. Moreover, the background is already quite small. We choose instead the more moderate cuts of $S_T > 1$ (1.5) TeV in the single electron (dielectron) channels.

Figures 9 - 11 show the lepton-jet invariant mass distributions where the \cancel{p}_T and S_T cuts have been applied. Again, a branching ratio $B = 0.5$ is assumed and the contributions from the dielectron and single electron channels are added. The same transverse-energy algorithm

as above is used to pair electron and jets. One notes that the QCD and $t\bar{t}$ backgrounds have practically vanished thanks to the p_T and S_T cuts, leaving the leptoquark signal virtually background-free. With this in mind, the 5σ statistical significance we require is trivially satisfied. The only requirement left is on the number of events, which is once again taken to be five.

While the background is seen to be negligible in the low-mass regime, the $t\bar{t}$ background reappears at higher values of the lepton-jet invariant mass, see Fig 9 (c-d) and Figs. 10-11 (e-f). However, the absence of correlation in the invariant mass M_{ej} for this background combined with a clean and rather narrow peak in the leptoquark signal allows the 5σ requirement to be satisfied.

One comment is in order regarding the invariant distributions of Figs. 9 - 11 (a). We see that the leptoquark mass peak is accompanied by a smeared bump at higher values of the invariant mass for low-mass leptoquark. This feature can be explained by the use of the transverse energy as criteria for lepton-jet pairing. This method works better when the kinematic limit for leptoquark production is approached. Leptoquarks of lower mass are generally emitted with much higher transverse momentum and the corresponding lepton-jet pair is thus emitted with high p_T and small angular separation. The uncertainty on the transverse momentum is thus increased while the signature will consist of one electron-jet pair in one hemisphere and another pair in the opposite hemisphere. The ideal pairing algorithm in this case would be to pair each electron with the nearest-neighbor jet instead. Nevertheless, as the total cross section for leptoquark is very large in the low-mass region, this alternative is not necessary.

Let us now consider the leptoquark discovery reach at the LHC. Once again, Fig. 12 shows the partial cross section for leptoquark production. As above, we have integrated the lepton-jet invariant mass distribution around the leptoquark peak for the whole kinematic range of leptoquark masses. The bin width over which we integrate varies as the peak widens and we take

- $M_{LQ} \leq 500$ GeV: $\Delta M_{ej} = 100$ GeV
- 500 GeV $< M_{LQ} \leq 1$ TeV: $\Delta M_{ej} = 150$ GeV
- 1 TeV $< M_{LQ} \leq 1.5$ TeV: $\Delta M_{ej} = 200$ GeV
- $M_{LQ} > 1.5$ TeV: $\Delta M_{ej} = 250$ GeV.

The results are displayed in Fig. 12 (a-b) for the scalar and vector cases with branching ratios of $B = 0.5$ (1). The LHC luminosity is assumed equal to 10 fb^{-1} . The corresponding discovery limit for 5 events is illustrated by the dashed line in Fig. 12. We find a discovery reach for scalar leptoquarks of 1 (1.1) TeV with $B = 0.5$ (1). In the vector case, the corresponding reach is 1.3 (1.4) TeV for $\kappa = 0$ and 1.55 (1.65) TeV for $\kappa = 1$.

VII. SUMMARY

Summarizing, we have presented the results of a complete analysis of first-generation scalar and vector leptoquark pair production at the Tevatron and the LHC. Both the dielectron and the single electron channels are included in the simulations. The importance of the

various Standard Model backgrounds with the same signature is also evaluated. We found the gauge boson background ($W, Z + 2$ jets) to be dominant at the Tevatron, followed by the background from QCD processes. For the LHC however, the background is relatively small and dominated by QCD processes and $t\bar{t}$ production. The discovery limits are established by requiring a 5σ statistical significance as well as a minimum of 5 events in a one-year run. Considering an integrated luminosity of $\mathcal{L} = 100 \text{ pb}^{-1}$ ($\mathcal{L} = 2 \text{ fb}^{-1}$) at the Tevatron, the results show that scalar leptoquarks can be detected up to 175 (265) GeV depending on the branching ratio. Similar limits on vector leptoquarks are set to 235 (325) GeV in the minimal anomalous coupling case ($\kappa = 0$) and 290 (380) GeV in the gauge case ($\kappa = 1$). The LHC discovery potential for leptoquarks increases these limits to 1 TeV in the scalar case, and to 1.3 and 1.55 TeV for vectors with anomalous magnetic couplings $\kappa = 0$ and 1 respectively.

ACKNOWLEDGMENTS

This research was supported by the Natural Sciences and Engineering Research Council of Canada and by the Fonds pour la Formation de Chercheurs et l'Aide à la Recherche du Québec.

REFERENCES

- [1] B. Schrempp and F. Schrempp, Phys. Lett. **B153** (1985) 101 and references therein; J. Wudka, Phys. Lett. **B167** (1985) 337.
- [2] H. Georgi and S. L. Glashow, Phys. Rev. Lett. **32** (1974) 438; J. C. Pati and A. Salam, Phys. Rev. **D10** (1974) 275; Phys. Rev. Lett. **31** (1973) 661; S. Dimopoulos and L. Susskind, Nucl. Phys. **B155** (1979) 237; S. Dimopoulos, Nucl. Phys. **B168** (1980) 69; P. Langacker, Phys. Rep. **72** (1981) 185; G. Senjanović and A. Šokorac, Z. Phys. **C20** (1983) 255; R. J. Cashmore *et al.*, Phys. Rep. **122** (1985) 275.
- [3] J. C. Pati and A. Salam, Phys. Rev. **D10** (1974) 275.
- [4] M. Green and J. Schwarz, Phys. Lett. **B149** (1984) 117; E. Witten, Nucl. Phys. **B258** (1985) 75; D. Gross, J. Harvey, E. Martinec and R. Rohm, Phys. Rev. Lett. **54** (1985) 502; Nucl. Phys. M. B. Green, J. H. Schwarz and E. Witten, “Superstring Theory”, Cambridge University Press, New York (1987).
- [5] J. L. Hewett and T. Rizzo, Phys. Rep. **183** (1989) 193.
- [6] L. Abbott and E. Fahri, Phys. Lett. **B101** (1981) 69; Nucl. Phys. **B189** (1981) 547.
- [7] ALEPH Collaboration, D. Decamp *et al.*, Phys. Rept. **216** (1992) 253; DELPHI Collaboration, P. Abreu *et al.*, Phys. Lett. **B316** (1993) 620; L3 Collaboration, Adriani *et al.*, Phys. Rept. **236** (1993) 1; OPAL Collaboration, G. Alexander *et al.*, Phys. Lett. **B263** (1991) 123; M. A. Doncheski and S. Godfrey, hep-ph/9608368; G. Bélanger, D. London and H. Nadeau, Phys. Rev. **D49** (1994) 3140.
- [8] OPAL Collaboration, FREIBURG-EHEP-97-04 and hep-ex/9706003.
- [9] OPAL Collaboration, Eur. Phys. J. **C2** (1998) 441.
- [10] L3 Collaboration, CERN-EP-98-031.
- [11] M. A. Doncheski and S. Godfrey, Phys. Rev. **D51** (1995) 1040 ; D. London and H. Nadeau, Phys. Rev. **D47** (1993) 3742.
- [12] I. Abt *et al.* (H1 Collaboration), Nucl. Phys. **B396** (1993) 3; M. Derrick *et al.* (ZEUS Collaboration), Phys. Lett. **B306** (1993) 173; T Ahmed *et al.* (H1 Collaboration), Z. Phys. **C64** (1994) 545; S. Aid *et al.* (H1 Collaboration), Phys. Lett. **B353** (1995) 578; Phys. Lett **B369** (1996) 173.
- [13] C. Adloff *et al.*, H1 collaboration, Z. Phys **C74** (1997) 191.
- [14] J. Breitweg *et al.*, ZEUS collaboration, Z. Phys. **C74** (1997) 207.
- [15] F. Abe *et al.*, CDF Collaboration, Phys. Rev. Lett. **79** (1997) 4327; P. J. Wilson, CDF Collaboration, FERMILAB-CONF-97-241-E; H. S. Kambara, CDF Collaboration, CDF-PUB-EXOTIC-GROUP-4222 and hep-ex/9706026; P. Azzi, CDF Collaboration, FERMILAB-CONF-97-148-E.
- [16] B. Abbott *et al.*, D0 Collaboration, Phys. Rev. Lett. **80** (1998) 2051; B. Klima, D0 Collaboration, FERMILAB-CONF-97-329-E and hep-ex/9710019; B. Abbott *et al.*, D0 Collaboration, Phys. Rev. Lett. **79** (1997) 4321; J. A. Wightman, D0 Collaboration, FERMILAB-CONF-97-178-E and hep-ex/9706024.
- [17] D. M. Norman, D0 Collaboration, FERMILAB-CONF-97-224-E and hep-ex/9706027.
- [18] J. L. Hewett and S. Pakvasa, Phys. Rev. **D37** (1988) 3165; J. E. Cieza Montalvo and O. J. P. Éboli, Phys. Rev. **D50**, (1994) 331. J. Blümlein, E. Boos and A. Kryukov, Z. Phys **C76** (1997) 137.
- [19] M. de Montigny, L. Marleau, G. Simon, Phys. Rev. **D52**, (1995) 533.

- [20] J.L. Hewett, T.G. Rizzo, S. Pakvasa, H.E. Haber and A. Pomarol , ANL-HEP-CP-93-52 and hep-ph/9310361 ; J.E. Cieza Montalvo and O.J.P. Eboli, Phys. Rev. **D50** (1994) 331; J. Blumlein, E. Boos and A. Kryukov, Z. Phys **C76** (1997) 137.
- [21] B. Heinemann, talk at the “DIS98, 6th International Workshop on DIS and QCD”, Brussels, April 4-9, 1998 (<http://www-h1.desy.de/h1/www/publications/hq2.html>); B. Straub, talk at the “Lepton-Photon '97 Conference” (http://www-zeus.desy.de/~ukatz/ZEUS_PUBLIC/hqex/hqex_highx.html).
- [22] F. Paige and S. Protopopescu, “Supercollider Physics”, World Scientific (1986); H. Baer, F. Paige, S. Protopopescu and X. Tata, “Proceedings of the Workshop on Physics at Current Accelerators and Supercolliders”, Argonne National Laboratory (1993).
- [23] B. Dion, L. Marleau and G. Simon, Phys. Rev. **D56** (1997) 479.
- [24] B. Dion, L. Marleau, G. Simon and M. de Montigny, Eur. Phys J **C2** (1998) 497.
- [25] O.J.P. Eboli, R.Z. Funchal, T.L. Lungov, Phys. Rev. **D57** (1998) 1715.
- [26] J.E.Cieza Montalvo, O.J.P. Eboli, M.B. Magro and P.G. Mercadante, IFT-P-030-98 and hep-ph/9805472.
- [27] W.W. Armstrong *et al.*, ATLAS Technical Proposal, CERN/LHCC/94-43 (1994).
- [28] G.L. Bayatian *et al.*, CMS Technical Proposal, CERN/LHCC/94-38 (1994).
- [29] H. Plothow-Besh, Comput. Phys. Commun. **75** (1993) 396.
- [30] M. Kramer, T. Plehn, M. Spira and P.M. Zerwas, Phys. Rev. Lett. **79** (1997) 341.
- [31] D0 Collaboration, “The D0 collaboration at the TeV33”, D0-NOTE-3410 and hep-ex/9804011.

FIGURES

FIG. 1. Feynman diagrams for leptoquark pair production via $q\bar{q}$ annihilation and gluon fusion.

FIG. 2. Examples of Feynman diagrams for (a) Z^*jj , (b) W^*jj , (c) QCD processes and (d) $t\bar{t}$ production.

FIG. 3. Missing p_T (\cancel{p}_T) distribution in the single electron channel at the Tevatron, with a branching ratio $B(LQ \rightarrow eq) = 0.5$. The vector leptoquark signal ($\kappa = 1$) is displayed for masses $M_{LQ} = 160, 200$ and 240 GeV along with the background from $W, Z +$ jets and QCD processes.

FIG. 4. Total transverse energy (S_T) distribution at the Tevatron, with a branching ratio $B(LQ \rightarrow eq) = 0.5$. Contributions from the dielectron and single-electron channels have been added and a missing transverse energy cut of $\cancel{p}_T \geq 40$ GeV has been applied to events in the single-electron channel. The vector leptoquark signal ($\kappa = 1$) is displayed for masses $M_{LQ} = 160, 200$ and 240 GeV along with the background from $W, Z +$ jets and QCD processes.

FIG. 5. Distribution of the invariant mass of the lepton-jet pair for (a) scalar (b) vector with $\kappa = 0$ and (c) vector with $\kappa = 1$ leptoquarks and for the various backgrounds at the Tevatron. Contributions from the dielectron and single-electron channels have been added and cuts have been applied on \cancel{p}_T and S_T .

FIG. 6. Partial cross section integrated around the leptoquark mass peak as a function of the invariant mass of the electron-jet pair for scalar and vector ($\kappa = 0, 1$) leptoquarks and for the various backgrounds at the Tevatron with (a) $B(LQ \rightarrow eq) = 0.5$ and (b) $B(LQ \rightarrow eq) = 1$. Kinematic cuts have been applied on \cancel{p}_T and S_T . The dash-dotted (dash-dot-dotted) lines correspond to the observation of 5 events considering a luminosity of 100 pb^{-1} (2 fb^{-1}).

FIG. 7. Missing p_T (\cancel{p}_T) distribution in the single electron channel at the LHC, with a branching ratio $B(LQ \rightarrow eq) = 0.5$. The vector leptoquark signal ($\kappa = 1$) is displayed for masses $M_{LQ} = 750, 1000$ and 1250 GeV along with the background from QCD processes and $t\bar{t}$ production.

FIG. 8. Total transverse energy (S_T) distribution at the LHC, with a branching ratio $B(LQ \rightarrow eq) = 0.5$. Contributions from the dielectron and single-electron channels have been added and a missing transverse energy cut of $\cancel{p}_T \geq 200$ GeV has been applied to events in the single-electron channel. The vector leptoquark signal ($\kappa = 1$) is displayed for masses $M_{LQ} = 750, 1000$ and 1250 GeV along with the background from QCD processes and $t\bar{t}$ production.

FIG. 9. Distribution of the invariant mass of the lepton-jet pair for scalar leptoquarks of mass (a) 250, (b) 500, (c) 750 and (d) 1000 GeV and for the various backgrounds at the LHC. Contributions from the dielectron and single-electron channels have been added and cuts have been applied on \cancel{p}_T and S_T .

FIG. 10. Distribution of the invariant mass of the lepton-jet pair for vector leptoquarks with $\kappa = 0$ of mass (a) 250, (b) 500, (c) 750, (d) 1000, (e) 1250 and (f) 1500 GeV and for the various backgrounds at the LHC. Contributions from the dielectron and single-electron channels have been added and cuts have been applied on \cancel{p}_T and S_T .

FIG. 11. Same as Fig. 10 for vector leptoquarks with $\kappa = 1$.

FIG. 12. Partial cross section integrated around the leptoquark mass peak as a function of the invariant mass of the electron-jet pair for scalar and vector ($\kappa = 0, 1$) leptoquarks and for the various backgrounds at the LHC with (a) $B(LQ \rightarrow eq) = 0.5$ and (b) $B(LQ \rightarrow eq) = 1$. Kinematic cuts have been applied on \cancel{p}_T and S_T . The dash-dot-dotted lines correspond to the observation of 5 events considering a luminosity of 10 fb^{-1} .

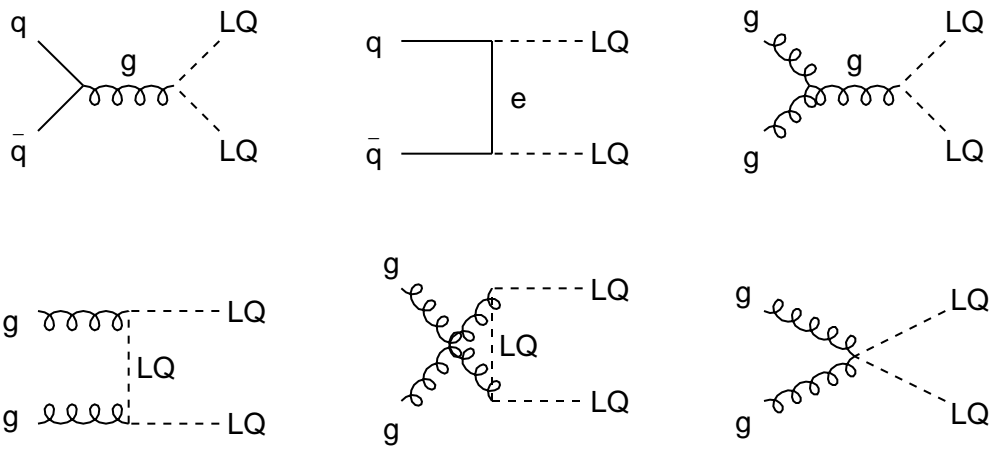


Fig. 1

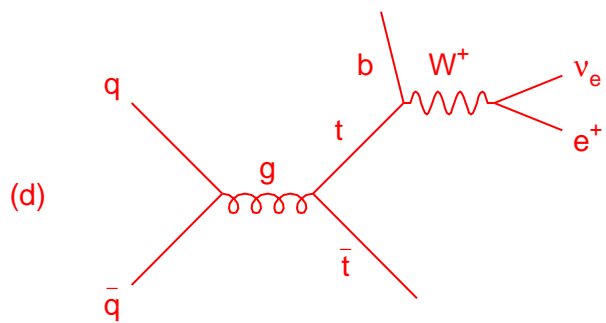
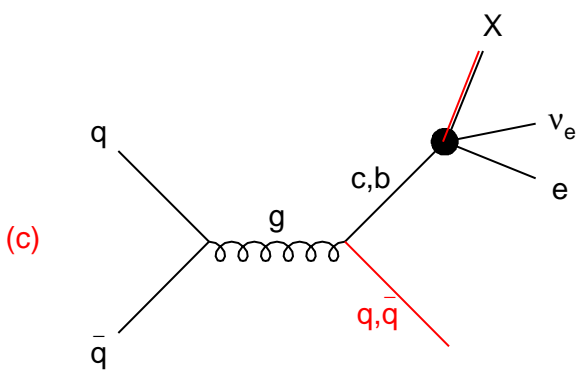
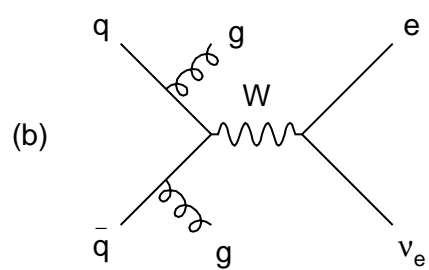
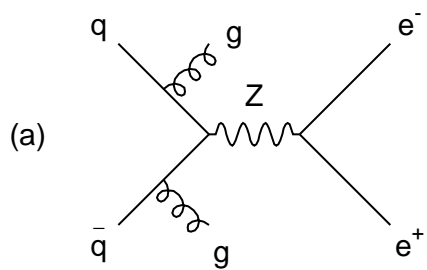


Fig. 2

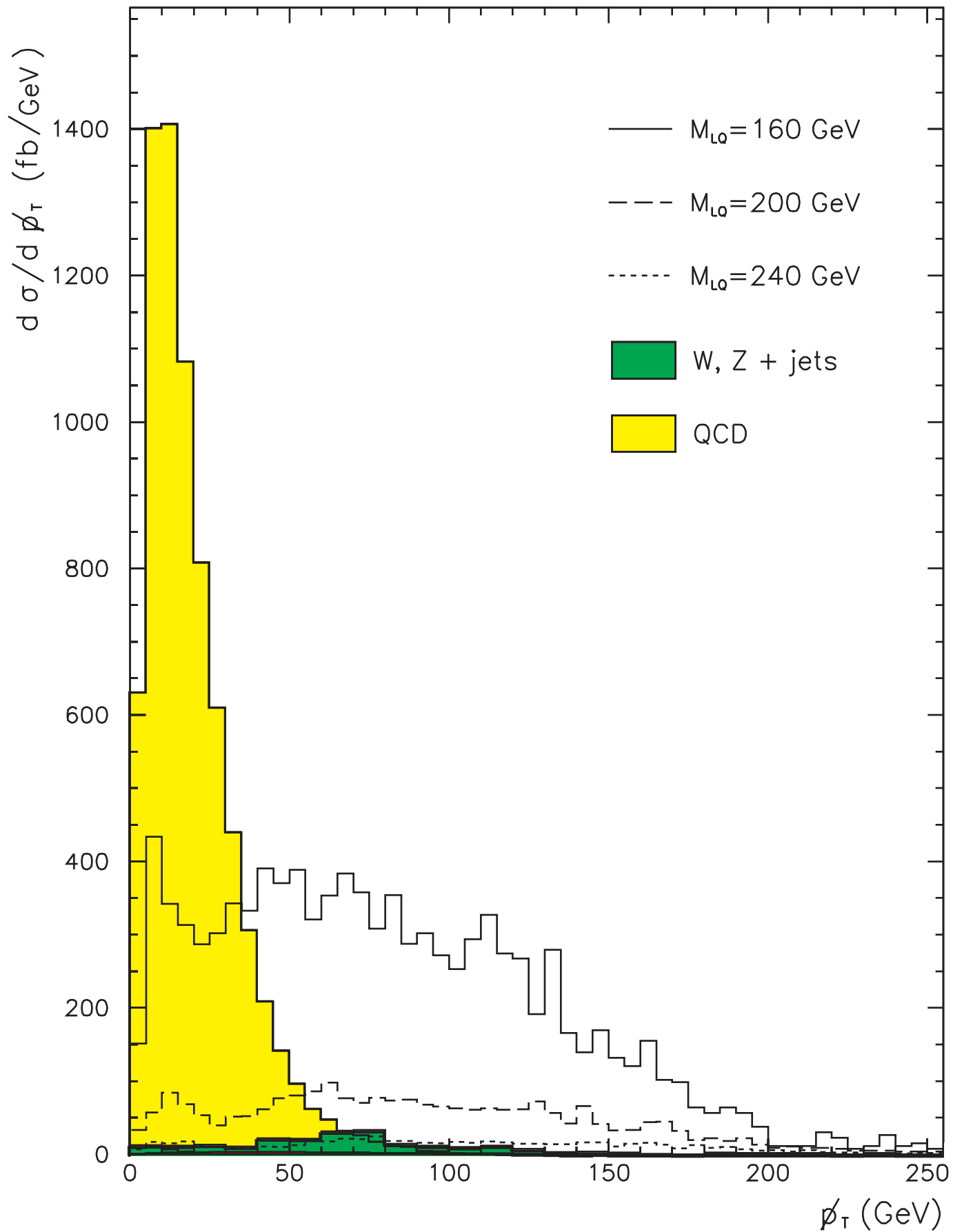


Fig. 3

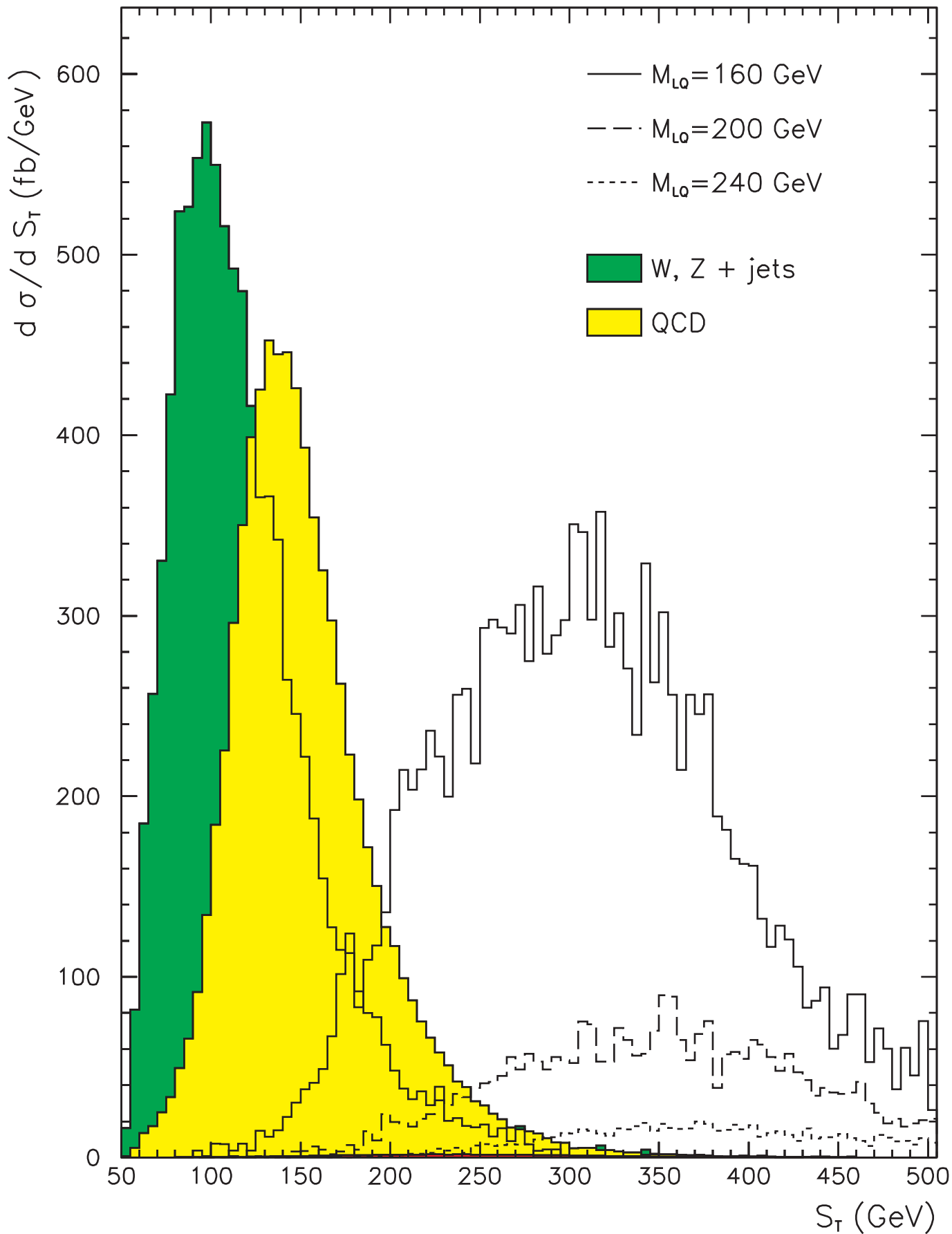


Fig. 4

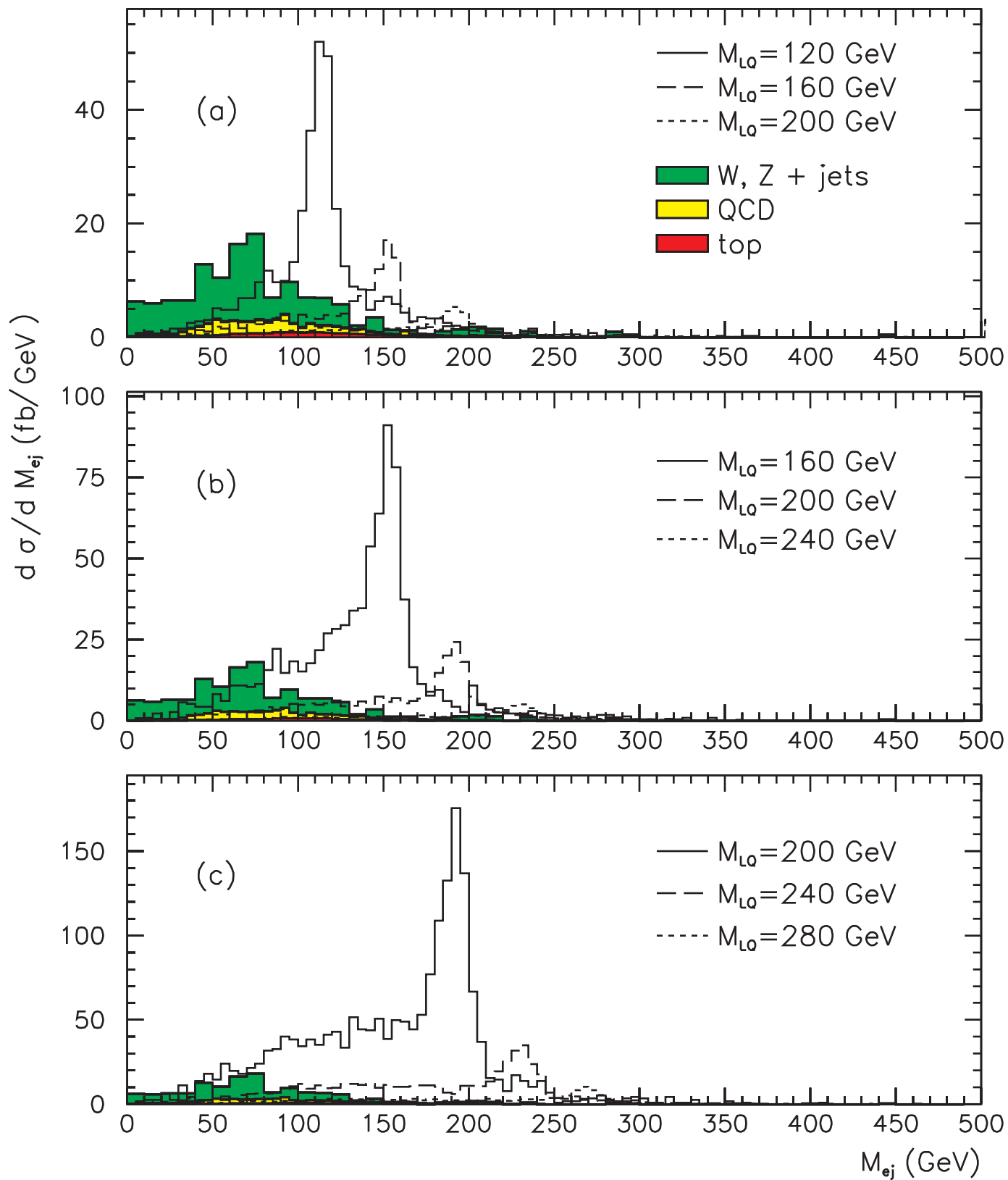


Fig. 5

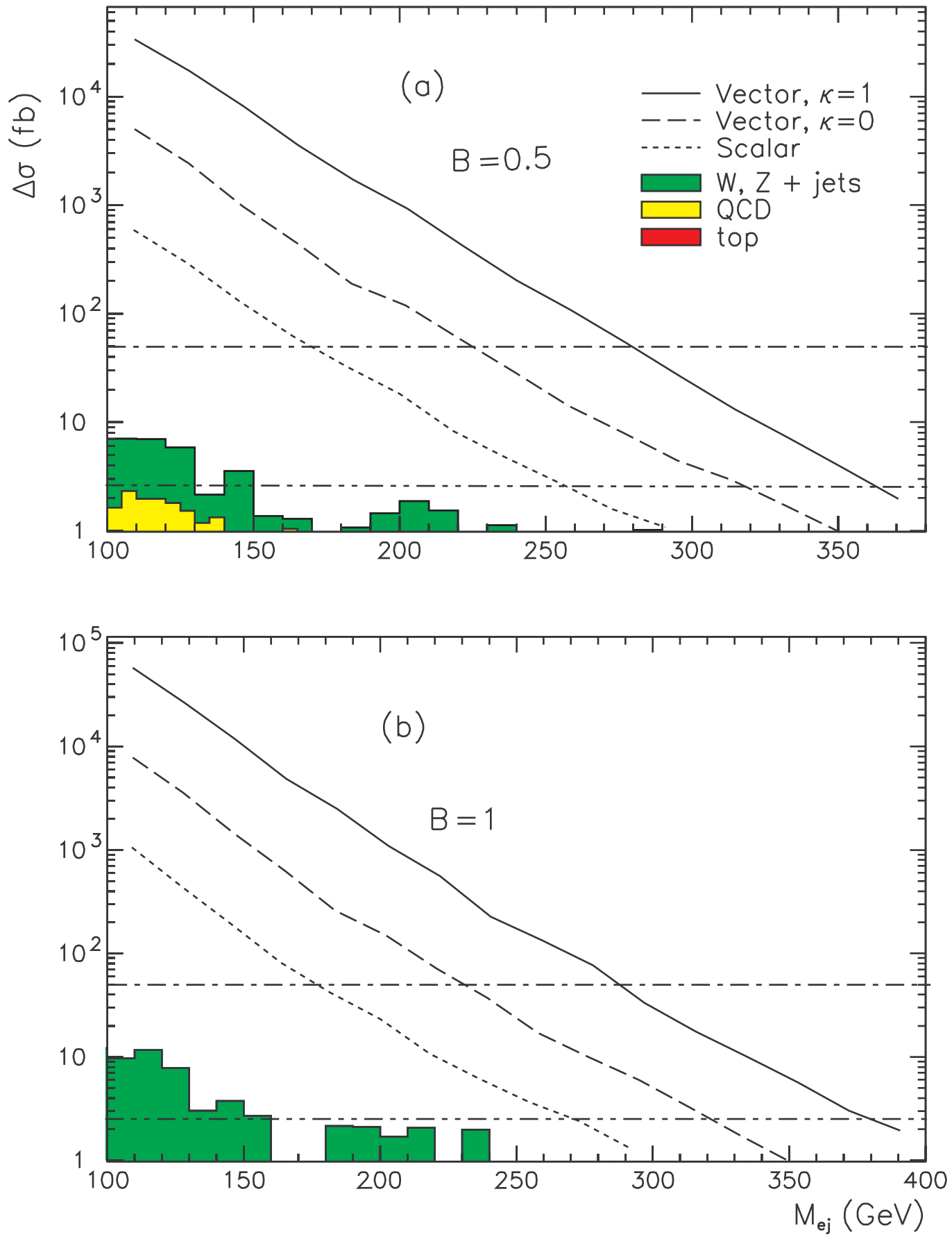


Fig. 6

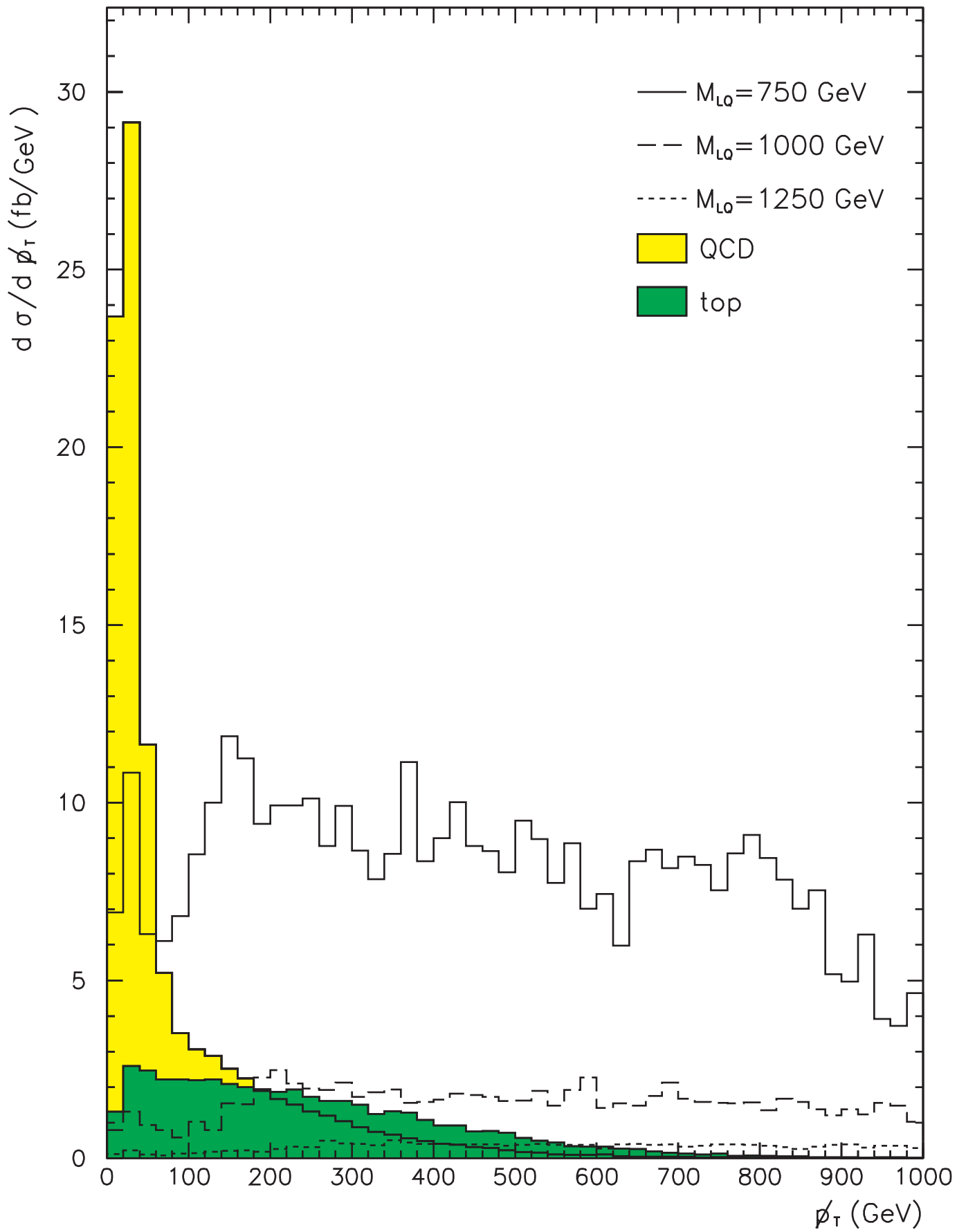


Fig. 7

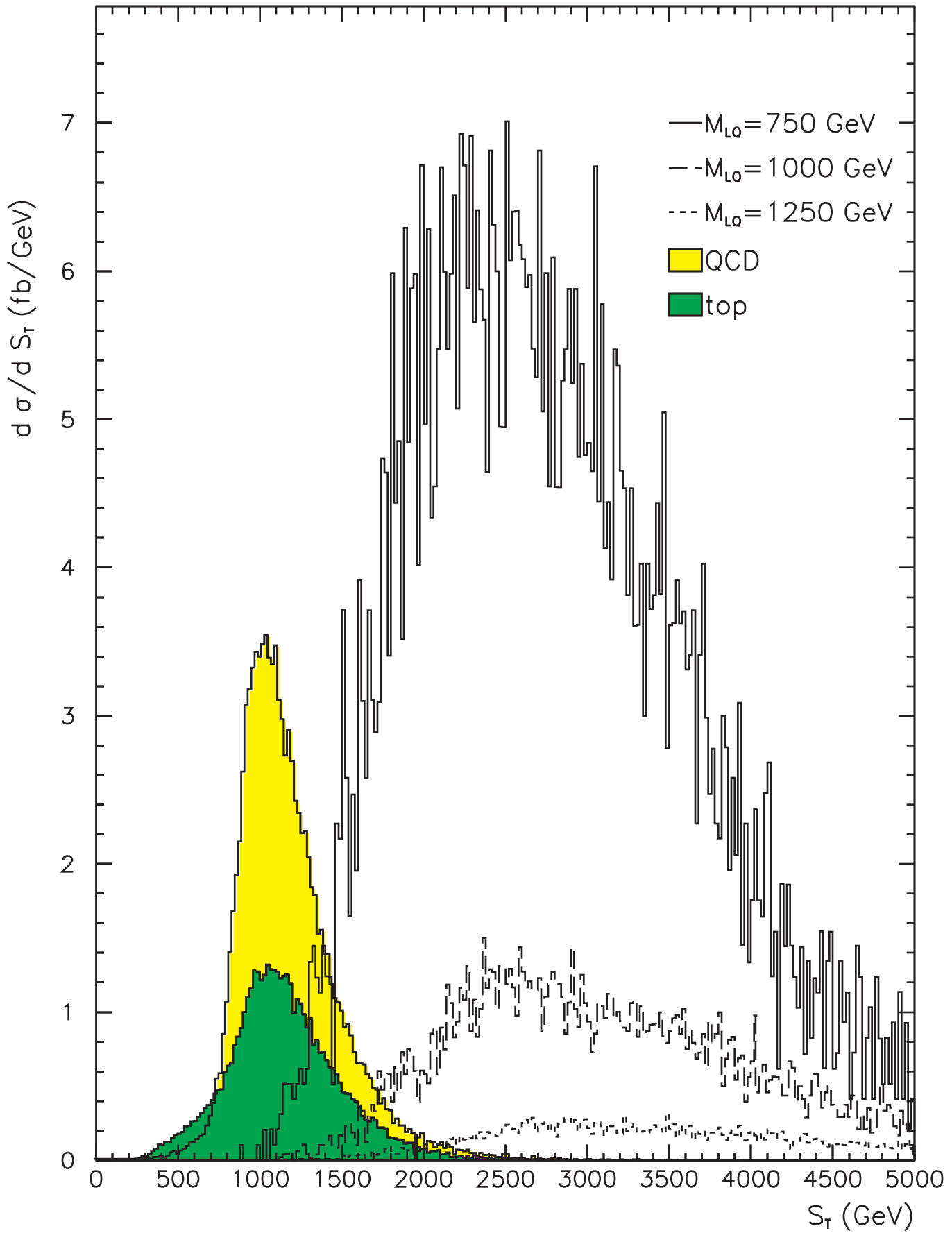


Fig. 8

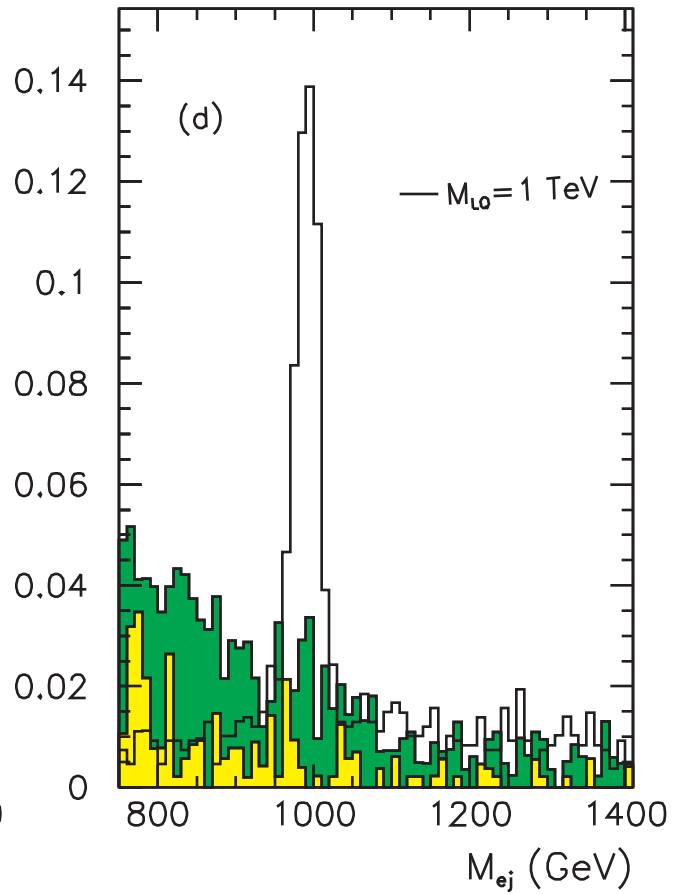
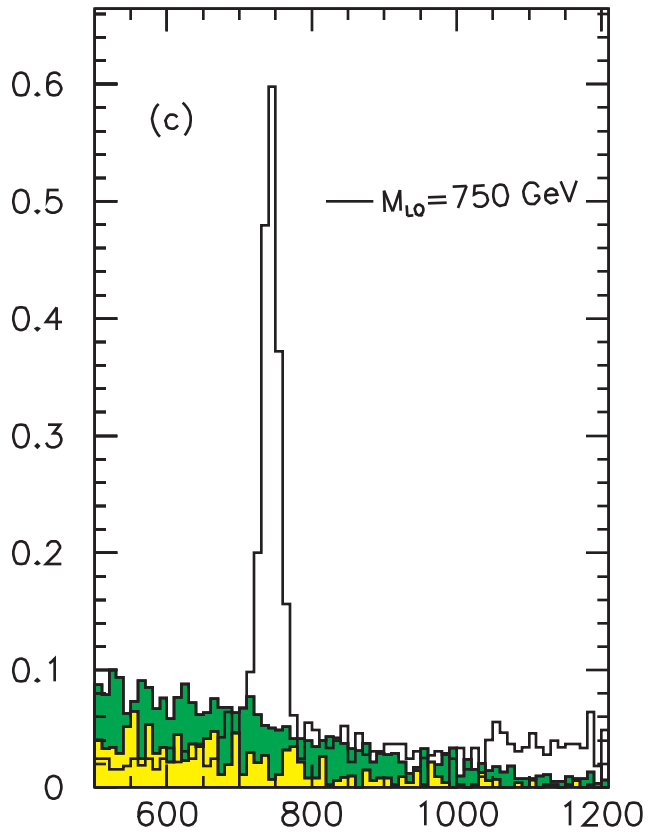
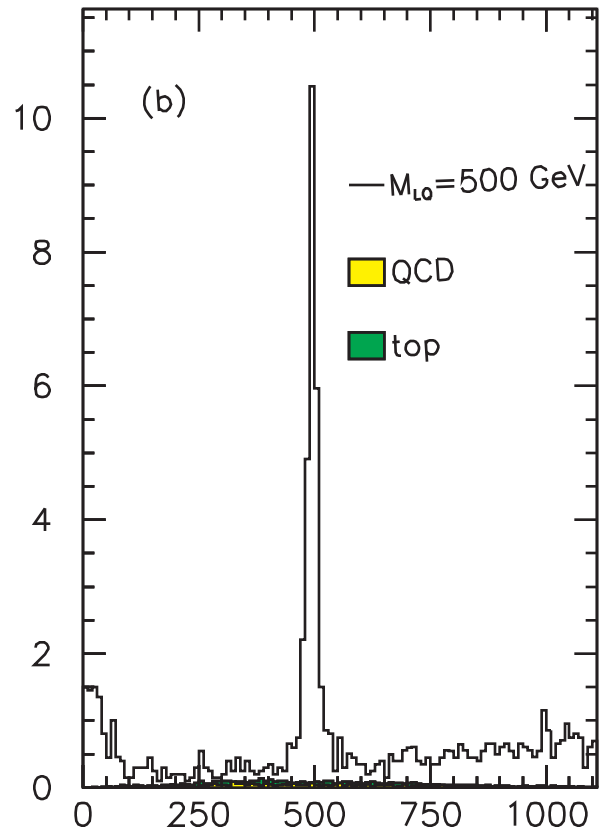
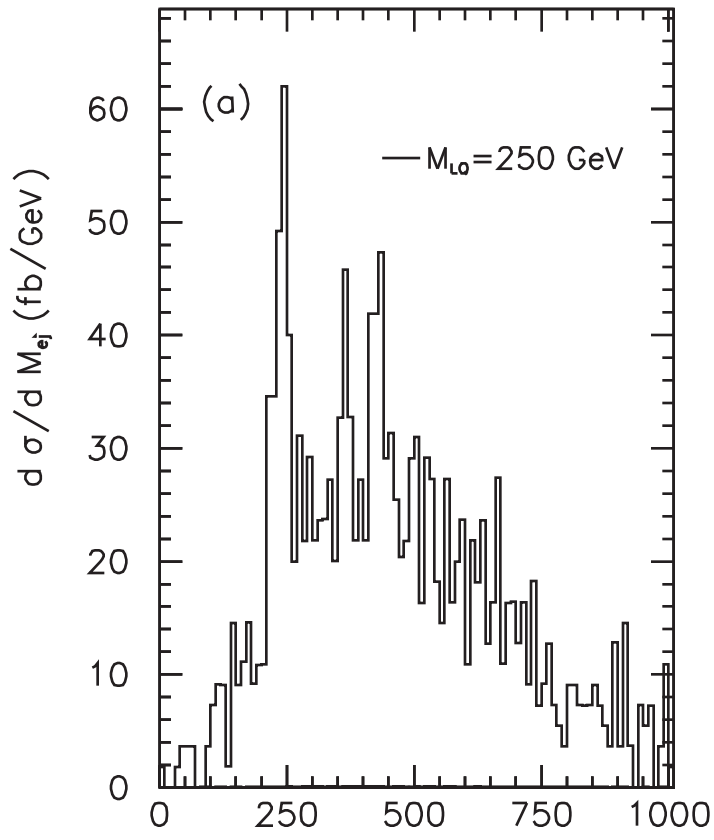


Fig. 9

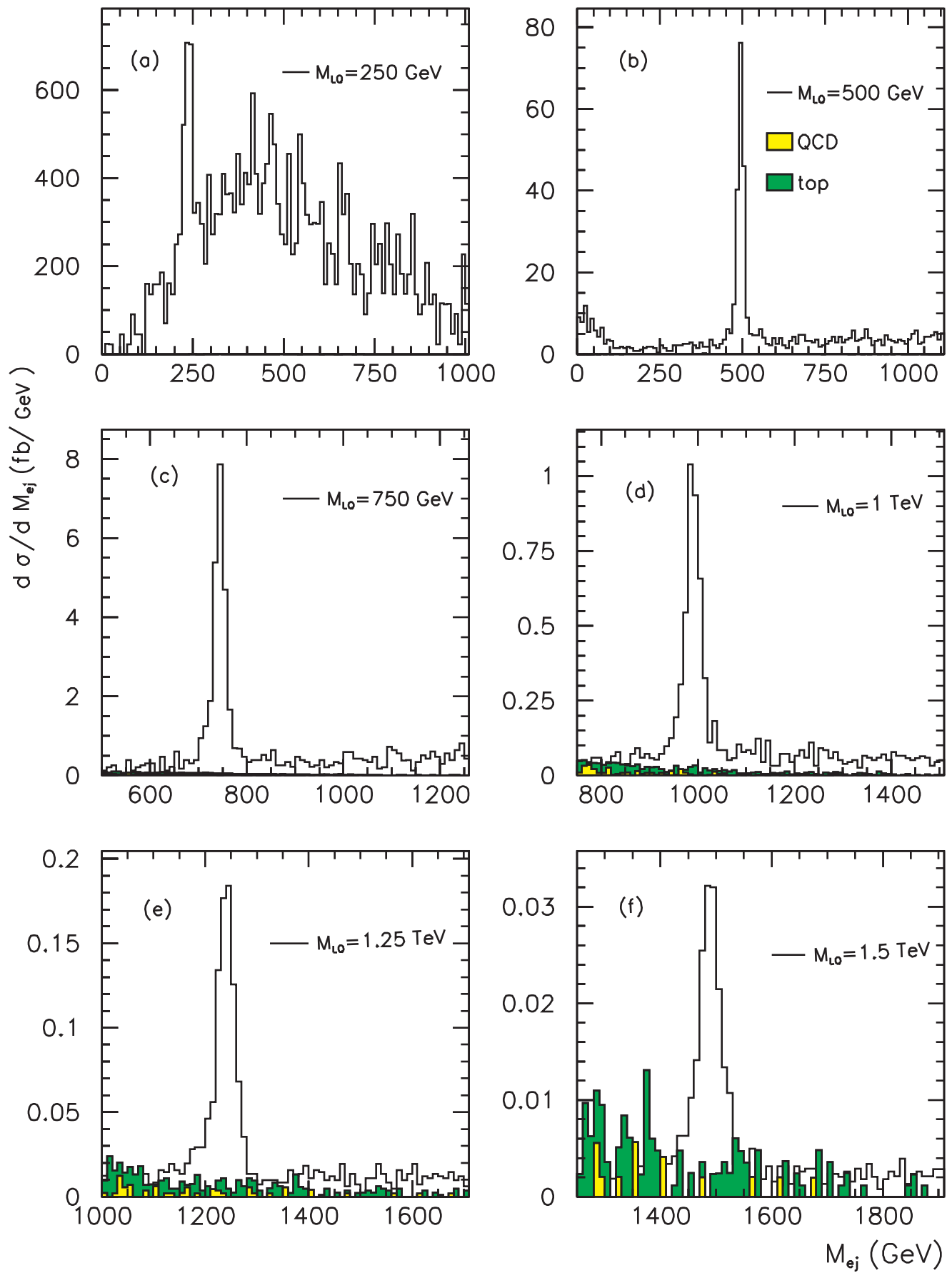


Fig. 10

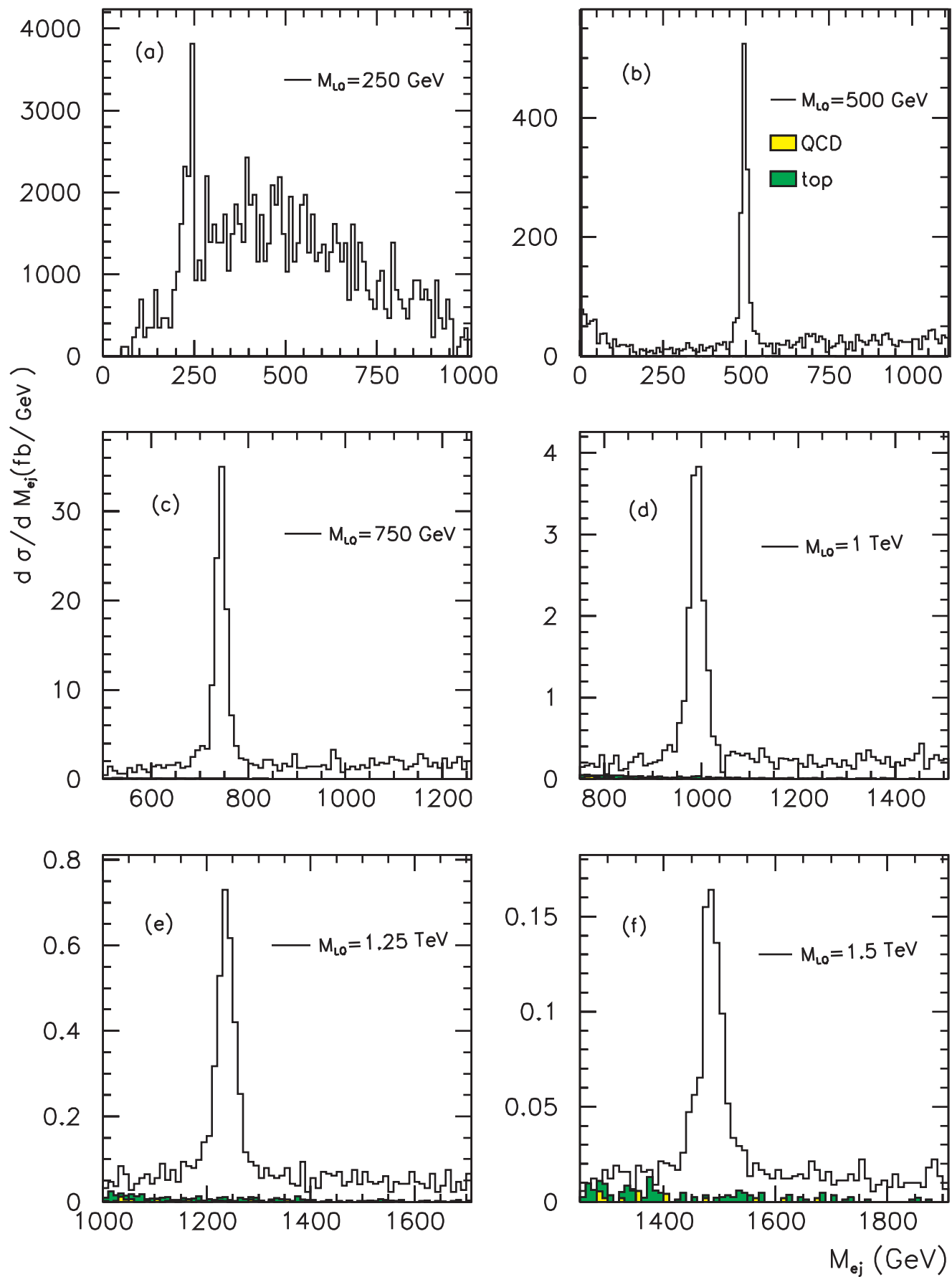


Fig. 11

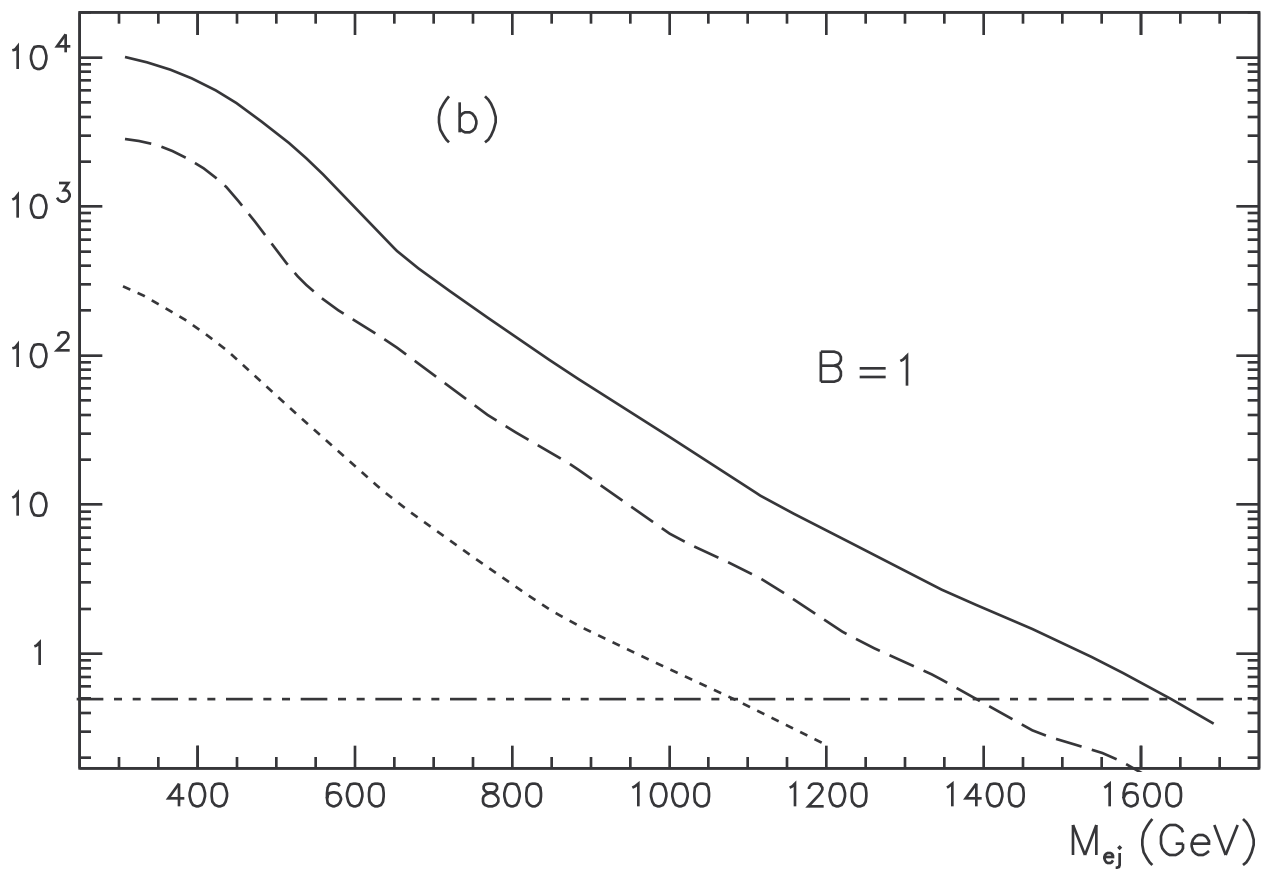
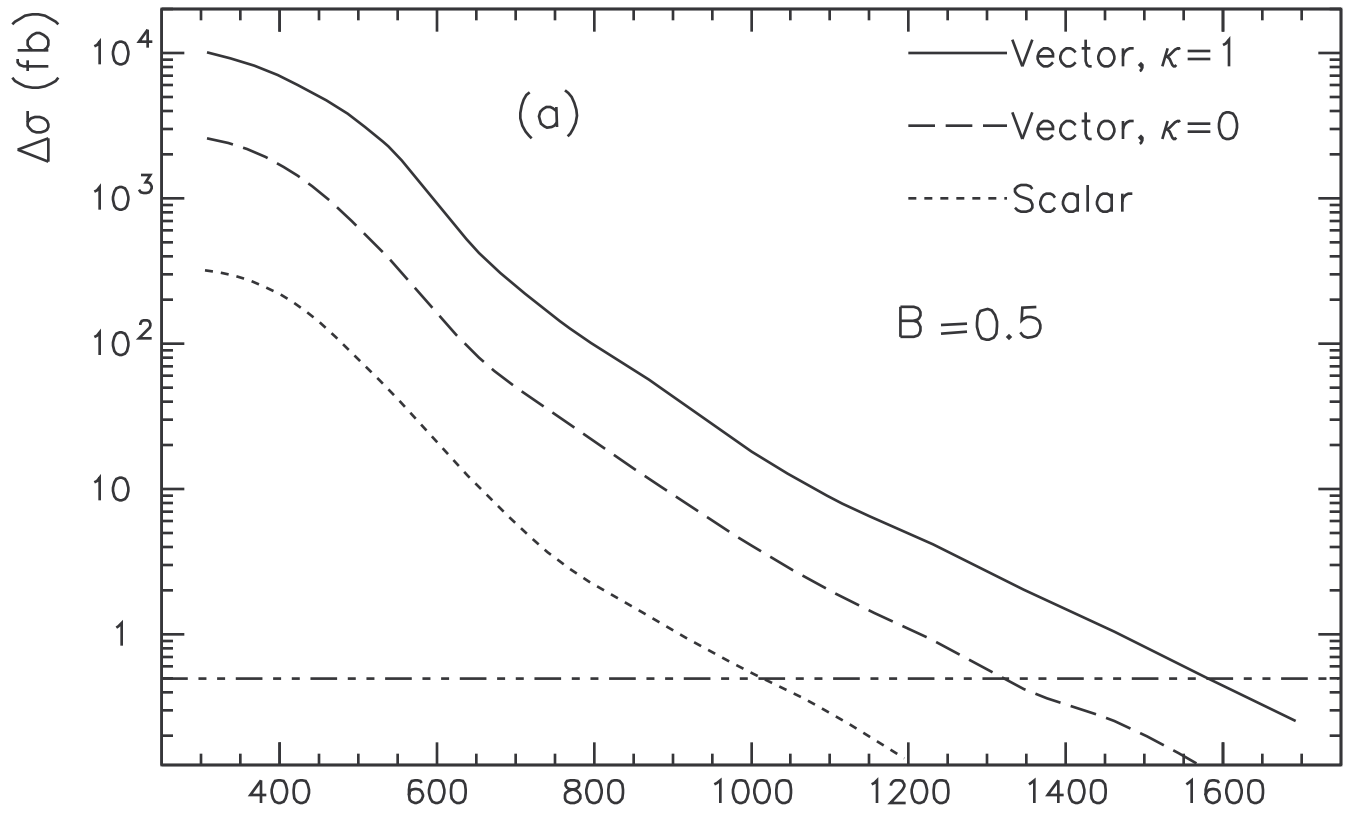


Fig. 12